

## Abstract

Exoplanet research has progressed to where direct observations are not only possible, but effective. Data from exoplanet observations provide insight into planetary system dynamics and evolution, and can be representative of local solar system processes. If present, the study of exoplanet atmospheres can provide further information about a system's composition and potential biosignatures. X-ray observations of exoplanets can detect atmospheric emission resulting from interaction with radiation and solar wind from the host star. The recently discovered terrestrial exoplanet, K Cancri b, is an excellent candidate for atmospheric analysis, due to similarities to the Earth–Sun system. Proposed observations with Chandra will attempt to detect, identify, and spectroscopically analyse K Cancri b's atmosphere, if present, leading to further research.

## Scientific Justification

When the Sun was initially proposed to be just a nearby star, scientists and philosophers began to be intrigued by the idea of exoplanets: planets beyond our solar system. In 1989, developments in telescope technology allowed for the first discovery of a planetary disk (*Historic*, 2019). This led to increased interest in the scientific potential of the field, and the development of instrumentation capable of furthering exoplanet research, such as the Hubble Space Telescope (HST) of 1990, and the Microvariability and Oscillation of Stars Telescope (MOST) of 2003 (*Historic*, 2019). The Spitzer Space Telescope followed MOST, after which came the incredibly successful Kepler mission—which discovered over 1000 exoplanets and provided a wealth of data to professional and amateur scientists eager to delve into the burgeoning field (*Historic*, 2019). The first exoplanets were confirmed in 1992, and atmospheric analysis conducted by 2001 (*Historic*, 2019). Light from exoplanets can now be detected through direct imaging, analysed spectroscopically, and even used to map surfaces and cloud cover (*Historic*, 2019). Beyond direct imaging, other techniques for exoplanet observation include (but are not limited to): the transit method, where periodic dips in the host star's light indicates the presence of a large body passing across its disk; gravitational pull detection through radial velocity Doppler effects, where the orbiting exoplanet causes a wobble in the host star; and, gravitational microlensing, where systems of massive bodies bend the light of distant objects in identifiable patterns (Ryden & Peterson, 2010, pp. 294-303).

By these methods, the study of exoplanets has been significant for revealing properties of planetary and stellar evolution. Particularly relevant is the changing composition of elements present in these systems, due to regularly occurring astrophysical processes such as accretion disk development, supernovae, and cluster aging (*Exoplanet Research*, 2019; *Exoplanets*, 2019). Additionally, this research contributes to a greater philosophical and biological understanding of the Universe, as atmospheric composition and planetary structure can provide insight into the origin and uniqueness of life (*Exoplanets*, 2019). Developments in these fields could be key to understanding the local solar system and Milky Way galaxy, and what to expect as these systems evolve. Continued contributions could result in the discovery of an array of directly observable Earth-like exoplanets at different stages of evolution, illuminating the changing composition, structure, and dynamics of terrestrial bodies (Ionov & Shematovic, 2015). Though difficult to detect, the presence of relatively small, terrestrial exoplanets makes for exciting discoveries.

Exoplanet atmospheres can be detected as well, by using X-ray observations to search for interactions between high-energy solar output and any gaseous envelope that is present. Solar output can be in the form of X-ray photons or solar wind. For example, X-rays emanating from the exceptionally hot (on the order of  $10^6$  K) solar corona of the Sun vary on its 11-year magnetic timescale, and fluctuate in maximum output by a factor of up to  $10^2$  (*The Sun*, 2014). Simultaneously, the solar wind bombards the solar system with a steady stream of energetic electrons, protons, heavy ions, and helium nuclei (Gallo, 2019). After being ejected from the Sun, these particles can be measured passing near the Earth with average velocities of around 400 km/s, and a mass density of about  $10^{-21}$  kg/m<sup>3</sup> (Ryden & Peterson, 2010, p. 178), making them significant contributors to detectable atmospheric interactions. For exoplanets that possess atmospheres, the study of analogous interactions can be particularly enlightening, providing insight into the overall

evolutionary state of the host system. Chemical composition can be determined through spectral analysis of the photon energies being emitted by the atmosphere in response to solar output, and used to identify physical processes that are occurring.

A key example of a terrestrial planet, the Earth features distinct solar output interaction processes (shown in Figure 1) that lead to X-ray emission: auroral (Bremsstrahlung); non-auroral (Thomson scattering and fluorescence); and geocoronal (exosphere Lyman- $\alpha$  emission, and solar wind charge exchange (SWCX)) (Waldrop & Paxton, 2013). These phenomena are well studied in the local solar system, and would be easily recognised if X-ray emission were to be detected from an exoplanet atmosphere. Spectroscopic analysis of these emission types, and a direct comparison to dynamic Earth processes, could provide insight into exoplanet magnetic field properties, chemical composition, and biosignatures indicating the potential for life. A description of these processes follows:

- **Auroral emission:** The primary source of X-ray emission from the Earth is that of aurorae (Bhardwaj et al., 2007). In the presence of a magnetic field, and with consistent radiation from the host star, aurorae emit nearly constantly and thus are excellent for atmospheric X-ray detections. Low energy aurorae are partially caused by processes in the Earth's magnetosphere that send charged particles falling onto the upper atmosphere, where they impart their energy via electron ionisation and collisions (Bhardwaj et al., 2007). Bremsstrahlung (free-free emission) is also present in low-energy aurorae, but is the main source of high-energy auroral emission (above 3–4 keV) (Bhardwaj et al., 2007). Bremsstrahlung occurs when accelerated electrons from the magnetosphere follow magnetic field lines to decelerate in the upper atmosphere, producing aurorae (Bhardwaj et al., 2007). In the visible spectrum, auroral based emission lines for oxygen— $5.577 \times 10^{-5}$  cm (green) and  $6.300 \times 10^{-5}$  cm (red)—correspond to low energies of about  $2 \times 10^{-6}$  keV (Tuttle, 2014). However, overall auroral emission spans a spectral range from visible to X-ray photons many keV in strength, and common inner-shell line emission for the Earth's atmosphere—nitrogen (K $\alpha$  at 0.393 keV), oxygen (K $\alpha$  at 0.524 keV), and argon (K $\alpha$  at 2.958 keV, K $\beta$  at 3.191 keV)—are all in the soft X-ray range (Bhardwaj et al., 2007). With a mix of nitrogen, oxygen, and argon K lines evident around 3 keV, in addition to Bremsstrahlung, it is these features that are likely to be detected from emitting atmospheres. Previous geocentric orbital observations by the Chandra HRC-I satellite instrument and resultant models indicate an approximate peak detection rate up to  $5 \times 10^5$  photons/s/sr/cm<sup>2</sup>, for auroral emission from the Earth's atmosphere (Bhardwaj et al., 2007).
- **Non-auroral emission:** Thomson scattering and fluorescence are evident in the Earth's atmosphere at energies above 2 keV during solar flares, and below 2 keV even during non-flare periods (Bhardwaj et al., 2007). Thomson (coherent) scattering occurs when a relatively low energy photon ( $h\nu \ll m_e c^2$ ) collides elastically with an electron, imparting an oscillation that emits the same energy as the incident photon (Gallo, 2019). At the same time, fluorescence is primarily attributed to the X-ray absorption and subsequent de-excitation of nitrogen, oxygen, and argon, at around 3 keV (Bhardwaj et al., 2007). As these processes peak in similar energies as aurorae, and regardless of the relation to flare-up activity of the host star, it is possible that such an event could occur during, and contribute to, an observation. PIXIE, on board NASA's POLAR research satellite observing the Earth's atmosphere, has confirmed brief intervals of such phenomena at intensities up to  $2 \times 10^4$  photons/s/sr/cm<sup>2</sup> (Petrinec et al., 2000).
- **Geocoronal emission:** Neutral hydrogen in the Earth's exosphere is illuminated in hard UV and soft X-rays, due to fluorescent Lyman- $\alpha$  emission and SWCX (Waldrop & Paxton, 2013; Bhardwaj et al., 2007). Lyman- $\alpha$  emission is detectable in the UV band, at a wavelength of  $1.216 \times 10^{-5}$  cm, or about 0.01 keV (Waldrop & Paxton, 2013). However, SWCX, where heavy ions from the solar wind strip electrons from neutral geocoronal material and then de-excite, causes emission proportional to heliosphere solar wind intensity in the soft X-ray band, peaking at less than 1 keV (Gallo, 2019; Bhardwaj et al., 2007; Gacesa, 2011). Observations of the Earth's geocorona indicate a detection rate on the order of  $10^{-1}$  photons/s/sr/cm<sup>2</sup> (Kameda et al., 2017; Koutroumpa, 2006). Though weak in

intensity, geocoronal emission cannot be completely discounted as a potential candidate for atmospheric X-ray detections.

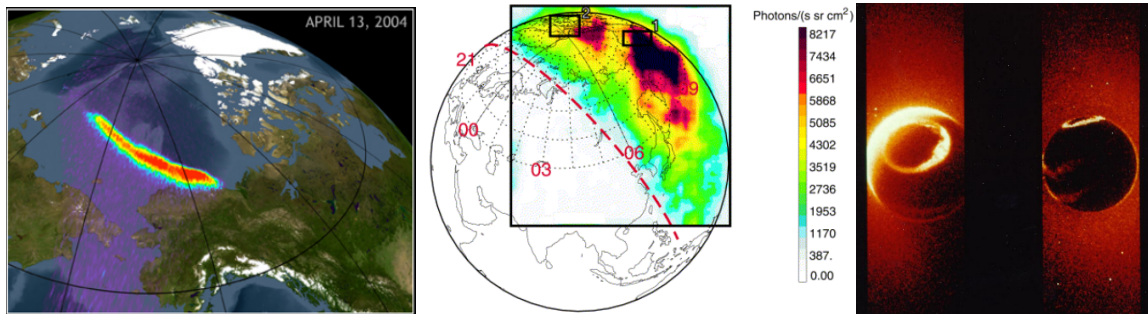


Figure 1. Previously observed data for auroral (left), non-auroral (centre), and geocoronal (right) emission. Adapted from Bhardwaj et al., 2007.

### K Cancri b

Recently, a revolutionary inner-system direct imaging detection uncovered a significantly Earth-like exoplanet orbiting the Sun-like G2V star, 'K Cancri a,' at a distance of 1.62 pc from the Earth, in Cancer. As expected of a G2V star, initial observations indicate that K Cancri a features an absolute magnitude of +4.6, effective temperature of 5810 K, mass of 1.04 solar masses, and radius of 1.04 solar radii (Ryden & Peterson, 2010, p. 579). The exoplanet, named 'K Cancri b,' follows a nearly circular orbit (eccentricity of 0.02) of approximately 2.53 AU in radius, at an inclination of only  $2^\circ$ , nearly face on to the observer (Ryden & Peterson, 2010, p. 298). By the small angle formula, the angular separation of the exoplanet and host star is about 1.6 arcseconds; observation is only barely achievable with current instrumentation and masking techniques to block the host star (Seager & Deming, 2010). Gravitational analysis of the K Cancri system indicates that it is likely a terrestrial body of about 1.28 Earth masses. The relative proximity and orientation of this system makes it ideal for directly observing K Cancri b's atmosphere, if it exists. Furthermore, assuming K Cancri b's rotational axis is approximately level with the plane of its system, this orientation is ideal for observations of auroral activity that takes place in the auroral oval, near the poles (Bhardwaj et al., 2007). As a similar system to that of the Earth-Sun, a direct comparison could be made; after identifying the presence of an atmosphere on K Cancri b, spectral analysis of X-ray emission could then suggest chemical composition, leading to deductions as to the planet's current evolutionary period, magnetic field properties, and potential biosignatures.

### Immediate Research Objectives

A minimum of 1 Ms of observation time is proposed to detect and identify atmospheric emission. In the presence of consistent emission (aurorae), data will be analysed spectroscopically for chemical composition, leading to additional research. Details follow:

- By simply seeking an X-ray detection of any type, the presence of an atmosphere can be confirmed, leading to further study. Observed data will be compared to Earth-based empirical observations (PIXIE, XMM-Newton, Chandra, HEAO-1, etc.) and models for terrestrial atmospheric interactions with solar output, mainly: auroral, non-auroral, and geocoronal emission. Key identifying spectral features of each process should be evident in the observed spectrum, including: prominent K-lines (up to  $\sim 3$  keV) and Bremsstrahlung (up to 10 keV), for aurorae; argon fluorescence ( $\sim 3$  keV) and Thomson scattering (up to 10 keV), for non-auroral emission coincident with flare-ups; and, geocoronal SWCX (primarily  $< 1$  keV) in the presence of a significant solar wind. Successful identification will provide information as to the dynamic properties of K Cancri b's magnetic field and atmosphere (Bond et al., 2010).

- In addition to the detection and identification of terrestrial atmospheric X-ray emission, as above, subsequent spectroscopic analysis will provide the chemical composition of K Cancri b's atmosphere. An Earth-based comparison of the proportions of common elements will provide further insight into natural processes occurring in the atmosphere, and indicate potential geological and biological functions below. This evidence will impart a better understanding of the evolution of the K Cancri system (Bond et al., 2010), including proto-planetary disk composition, evolving system dynamics, and biosignatures that indicate the potential for life.

### Technical Justification

The versatile spectroscopy instruments of the Chandra spacecraft are ideal for difficult direct observations of this type. The Advanced CCD Imaging Spectrometer (ACIS-S), coupled with the High Energy Transmission Grating (HETG), will provide a broad range of detection that covers all three atmospheric emission processes described above. This range, coupled with excellent angular and spectral resolution, and high-efficiency pointing accuracy and stability, makes Chandra the best candidate for precision observation of K Cancri b. Additionally, Chandra's angular resolution allows for a post-processing pixel mask that will filter obscuring detections from K Cancri a.

General specifications include four nested pairs of paraboloid and hyperboloid mirrors, a maximum field of view of 1 degree in diameter, angular resolution of 0.492 arcseconds per pixel, pointing stability (RMS) of 0.25 arcseconds over 95% of observation, pointing accuracy of 30 arcseconds over 99% of observation, and an effective detection area of 400 square cm at 1 keV (*Chandra*, 2014). Most relevant to this proposal, ACIS-S has an energy range of 0.2 – 10 keV, imaging resolution of 0.5 arcseconds, and a sensitivity of  $4 \times 10^{-15}$  ergs/s/cm<sup>2</sup> over 10<sup>5</sup> seconds of observation; additionally, the HETG features an energy range of 0.4 – 10 keV, with a spectral resolution of 60 – 1000 (*Chandra*, 2014).

Other observatories were considered, but found lacking for their resolution, spectroscopic abilities, or energy range. For example, XMM-Newton does not compare to Chandra's point-spread function (PSF) for resolving data; NICER is designed for neutron stars and does not meet the spectroscopic goals of the observation; NuSTAR is designed for hard X-rays observations; and, Swift and ASTROSAT are both too low in resolving power. Chandra is a NASA-operated X-ray telescope in a highly elliptical geocentric orbit of up to 139,000 km, and features four observing instruments for X-ray imaging and spectroscopy of high-energy regions of the Universe (*Chandra*, 2014).

Unfortunately, direct exoplanet observations suffer from low source flux (as will be detailed), and require long observation times. However, the relatively static configuration of the K Cancri system would allow for multiple short-duration exposures to be stacked without significantly affecting data quality. Therefore, it is suggested that portions of the following observation be performed during instrument down-time.

These exposures could be fit to current spaces in the Chandra schedule. Additionally, the nearly face-on relative orientation of K Cancri b's orbit (2°) allows for observation at any time, dependent only on Chandra's relative position to the target. Previous direct observations of distant Jovian exoplanets have achieved good spectral resolution with long durations, as is necessary for the flux relationship to the inverse-square law (Marin & Grosso, 2017). To demonstrate the need for this long-duration exposure, simulations were modelled using NASA HEASARC WebPIMMS and WebSpec software.

Assuming an average orbital distance of  $1 \times 10^{-9}$  pc for the POLAR observations, a flux ratio of  $3.81 \times 10^{-19}$  is found for similar processes present on K Cancri b, at a distance of 1.62 pc. Thus, local approximate peak photon counts (as described) for auroral, non-auroral, and geocoronal emission convert into K Cancri values of  $1.90 \times 10^{-13}$ ,  $7.62 \times 10^{-15}$ , and  $3.81 \times 10^{-20}$  ergs/s/cm<sup>2</sup>, respectively. Thus, assuming predominantly auroral emission for the given source flux, WebPIMMS predicts a count rate of  $1.022 \times 10^{-3}$  counts/s, no significant pile-up, and a normalisation factor of  $4.164 \times 10^{-5}$  for the HEG1 (sum of +1 and -1 detections) grating (*Tools*, n.d.). Then, using the given WebPIMMS parameters for

HEG1, WebSpec simulated Bremsstrahlung spectra were created to determine the minimum proposed observation time of 1 Ms, necessary to resolve immediate objective features. The estimated parameter constraints provide an acceptable fit to the proposed model, evident in the simulation outcomes of Figure 2:

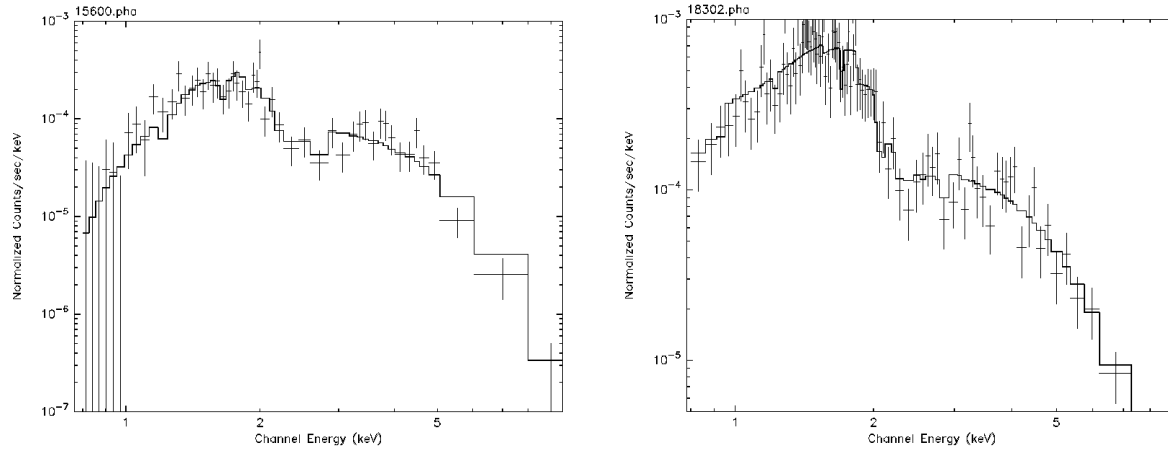


Figure 2. Simulated WebSpec Bremsstrahlung spectrum for Chandra ACIS-S and HETG (HEG order +1 (left) and -1 (right)) with a peak temperature of 4 keV, normalisation for a source flux of  $1.90 \times 10^{-13}$  ergs/s/cm<sup>2</sup>, and total exposure time of 1 Ms. Parameter constraints provide an acceptable fit to proposed models. Adapted from Tools, NASA: HEASARC.

## Conclusions

Though exoplanet observations can be time consuming, it is important to consider the direct relevance of such data to local, terrestrial processes, and how these insights can contribute to the development of astrophysics and other relevant fields. The K Cancri and Earth-Sun systems are highly similar, meaning that study of the exoplanet will provide a glimpse into the history, connection, and future state of local dynamics. Furthermore, Chandra detections of atmospheric X-ray emission from K Cancri b could provide insight into planetary system dynamics, terrestrial processes, and stellar evolution. All of these contributions would provide much needed clarification as to the nature of local processes, how they originate, and what may happen next. The ACIS-S instrument, coupled with the HETG grating assembly and a post-processing pixel mask, is optimal for making such detections, with a requested minimum of 1 Ms of observation time necessary to resolve immediate objectives.

For millennia, the human race has sought a sense of purpose and identity in the cosmos, and the confirmation of a potential 'sister-system' through detected biosignatures would be a huge step towards both a philosophical and scientific understanding of this identity. If Chandra is successful in its observation, it could truly provide 'a whole new world' of knowledge to the scientific community.

## References

- Bond, J. C., O'Brien, D. P., & Lauretta, D. S. (2010). The compositional diversity of extrasolar terrestrial planets. *The Astrophysical Journal*, 715(2), 1050-1070. Retrieved from <https://iopscience-iop-org.library.smu.ca/article/10.1088/0004-637X/715/2/1050/pdf>
- Bhardwaj, A., Gladstone, R., Elsner, R. F., Østgaard, N., Waite, J. H. Jr., Cravens, T. E., Chang, S., Majeed, T. & Metzger, A. (2007). First terrestrial soft X-ray auroral observation by the Chandra X-ray Observatory. *Journal of Atmospheric and Solar-Terrestrial Physics*, 69(1-2), 179-187. Retrieved from <https://www-sciencedirect-com.library.smu.ca/science/article/pii/S1364682606002471>
- Bhardwaj, A., Elsner, R. F., Gladstone, R., Cravens, T. E., Lisse, C. M., Dennerl, K., Branduardi-Raymont, G., Wargelin, B. J., Waite, J. H. Jr., Robertson, I., Østgaard, N., Beiersdorfer, P., Snowden, S. L., & Kharchenko, V. (2007). X-rays from solar system objects. *Planetary and Space Science*, 55(9), 1135-1189. Retrieved from <https://www-sciencedirect-com.library.smu.ca/science/article/pii/S0032063306003370>
- Chandra X-ray observatory. (2014). *NASA*. Retrieved from <http://chandra.harvard.edu/index.html>
- Exoplanets. (2019). *ESA*. Retrieved from <http://sci.esa.int/exoplanets/60657-the-future-of-exoplanet-research/>
- Exoplanet Research Centre. (2019). *Cambridge University*. Retrieved from <https://exoplanets.phy.cam.ac.uk/research>
- Gacesa, M., Muller, H. R., Cote, R. & Kharchenko, V. (2011). Polarisation of the charge-exchange X-rays induced in the heliosphere. *The Astrophysical Journal Letters*, 732(21), 1-5. Retrieved from <https://iopscience-iop-org.library.smu.ca/article/10.1088/2041-8205/732/2/L21/pdf>
- Gallo, L. (2019). Class notes [PDF slides]. *Saint Mary's University*. Retrieved from <http://www.ap.smu.ca/~lgallo/A4600/>
- Historic timeline. (2019). *NASA*. Retrieved from <https://exoplanets.nasa.gov/alien-worlds/historic-timeline/>
- Ionov, D. & Shematovich, E. (2015). Hydrogen-dominated upper atmosphere of an exoplanet: Heating by stellar radiation from soft X-rays to extreme ultraviolet. *Solar System Research*, 49(5), 339-345. Retrieved from <https://link-springer-com.library.smu.ca/content/pdf/10.1134/S0038094615050056.pdf>
- Kameda, S., Ikezawa, S., Sato, M., Kuwabara, M., Osada, N., Murakami, G., Yoshioka, K., Yoshikawa, I., Taguchi, M., Funase, R., Sugita, S., Miyoshi, Y. & Fujimoto, M. (2017). Ecliptic north-south symmetry of hydrogen geocorona. *Geophysical Research Letters*, 44(23), 11,706-11,712. Retrieved from <https://agupubs-onlinelibrary-wiley-com.library.smu.ca/doi/pdf/10.1002/2017GL075915>
- Koutroumpa, D., Lallement, R., Kharchenko, V., Dalgarno, A., Pepino, R., Izmodenov, V. & Quémerais, E. (2006). Charge transfer induced EUV and soft X-ray emissions in the heliosphere. *Astronomy and Astrophysics*, 460, 289-300. doi: 10.1051/0004-6361:20065250
- Marin, F. & Grosso, N. (2017). Computation of the Transmitted and Polarized Scattered Fluxes by the Exoplanet HD 189733b in X-Rays. *The Astrophysical Journal*, 835(2), 1-13. Retrieved from <https://iopscience-iop-org.library.smu.ca/article/10.3847/1538-4357/835/2/283/pdf>
- Petrinec, S. M., McKenzie, D. L., Imhof, W. L., Mobilia, J., & Chenette, D. L. (2000). Studies of X-ray observations from PIXIE. *Journal of Atmospheric and Solar-Terrestrial Physics*, 62(10), 875-888. Retrieved from <https://www-sciencedirect-com.library.smu.ca/science/article/pii/S1364682600000353>
- Ryden, B. & Peterson, B. M. (2010). *Foundations of astrophysics*. Ohio: Pearson.
- Seager, S. & Deming, D. (2010). Exoplanet atmospheres. *Annual Review of Astronomy and Astrophysics*, 48(1), 631-672. Retrieved from <https://www.annualreviews.org/doi/full/10.1146/annurev-astro-081309-130837>
- The Sun as an X-ray source. (2014). *NASA*. Retrieved from <https://imagine.gsfc.nasa.gov/science/objects/sun2.html>
- Tuttle, S. (2014). Calculating the auroral electron energy. *Astronomy & Geophysics*, 55(4:1), 17-19. Retrieved from <https://doi.org/10.1093/astrogeo/at160>
- Waldrop, L. & Paxton, L. (2013). Lyman  $\alpha$  airglow emission: Implications for atomic hydrogen geocorona variability with solar cycle. *Journal of Geophysical Research: Space Physics*, 118(9), 5874-5890. Retrieved from <https://agupubs-onlinelibrary-wiley-com.library.smu.ca/doi/pdf/10.1002/jgra.50496>
- Tools. (n.d.). *NASA: HEASARC*. Retrieved from <https://heasarc.gsfc.nasa.gov/cgi-bin/Tools/>